Journal of Hazardous Materials 192 (2011) 299–306

Contents lists available at ScienceDirect

Journal of Hazardous Materials

journal homepage: www.elsevier.com/locate/jhazmat

# Interaction of silver nanoparticles (SNPs) with bacterial extracellular proteins (ECPs) and its adsorption isotherms and kinetics

S. Sudheer Khan, P. Srivatsan, N. Vaishnavi, Amitava Mukherjee, N. Chandrasekaran*

*Centre for Nano-Biotechnology, School of Bio-Sciences and Technology, VIT University, Katpadi Road, Vellore 632014, Tamilnadu, India*

ARTICLE INFO

*Article history:*
Received 23 December 2010
Received in revised form 31 March 2011
Accepted 9 May 2011
Available online 1 June 2011

*Keywords:*
Silver nanoparticles
Extracellular protein
Surface charge
Adsorption isotherms
Adsorption kinetics

ABSTRACT

Indiscriminate and increased use of silver nanoparticles (SNPs) in consumer products leads to the release of it into the environment. The fate and transport of SNPs in environment remains unknown. We have studied the interaction of SNPs with extracellular protein (ECP) produced by two environmental bacterial species and the adsorption behavior in aqueous solutions. The effect of pH and salt concentrations on the adsorption was also investigated. The adsorption process was found to be dependent on surface charge (zeta potential). The capping of SNPs by ECP was confirmed by Fourier transform infrared spectroscopy and X-ray diffraction. The adsorption of ECP on SNPs was analyzed by Langmuir and Freundlich models, suggesting that the equilibrium adsorption data fitted well with Freundlich model. The equilibrium adsorption data were modeled using the pseudo-first-order and pseudo-second-order kinetic equations. The results indicated that pseudo-second-order kinetic equation would better describe the adsorption kinetics. The capping was stable at environmental pH and salt concentration. The destabilization of nanoparticles was observed at alkaline pH. The study suggests that the stabilization of nanoparticles in the environment might lead to the accumulation and transport of nanomaterials in the environment, and ultimately destabilizes the functioning of the ecosystem.



## 1. Introduction

Silver nanoparticles (SNPs) with a size range of <100 nm have been used in many household and industrial products, such as in tires, textiles, cosmetics, food industries for packaging and processing, medical applications in wound care products, therapeutic devices, diagnostics and drug delivery [1–6]. The strong antimicrobial effect of silver to a wide range of microorganisms combined with its low toxicity to humans has led to the development of silver based products in many antibacterial applications [7]. There are more than 1000 nano-based consumer products [8] in market, of which silver nanoparticle incorporated consumer products, including clothing and cosmetics are about 200 [9]. The production rate of SNPs is estimated to be 500 tonnes/year [10].

The nanoparticle properties differ substantially from that of its bulk particles. Though nanoparticles are having numerous technological applications, at the same time they are hazardous to biological systems [11]. Studies on mammalian cell lines proved that SNPs enter the cell and cause cellular damage [12]. The SNPs are capable of inducing chromosomal aberrations, DNA damage and mitochondrial dysfunction [13]. SNPs induce toxicity to environmentally relevant bacterial species also [14,15]. The studies by Impellitteri et al. [16] revealed that the SNPs can easily leak into waste water during washing from SNP impregnated clothes and the washing systems, thus potentially disrupting beneficial bacteria used in waste-water treatment facilities, and the endangering aquatic organisms in lakes, streams and other fresh water systems. Blaser et al. [17] reported the release of SNPs to the sewage treatment plants and they are estimated to be 270 tonnes/year. Therefore, increased presence of silver nanoparticles in the environment requires a basic understanding about their interactions with biological molecules. The major objective of this study was to investigate the interaction of SNPs with bacterial extracellular proteins (ECPs). The ECP used in the present study was extracted from two bacterial species *Aeromonas punctata* and *Bacillus pumilus*, isolated from the environment. The study revealed the possible stabilization of nanoparticles in the environment, especially in the fresh water systems. The study also aimed to investigate (i) effect of pH and salt concentration on adsorption, (ii) the influence of surface charge on adsorption, and (iii) the adsorption isotherms and kinetics of adsorption of ECP onto SNPs.

## 2. Materials and methods

### 2.1. Materials

All chemicals and nanoparticles were obtained from Sigma–Aldrich, USA. All the experiments were carried out in

* Corresponding author. Tel.: +91 416 2202624.
*E-mail addresses:* nchandrasekaran@vit.ac.in, nchandra40@hotmail.com (N. Chandrasekaran).

0304-3894/$ – see front matter © 2011 Elsevier B.V. All rights reserved.
doi:10.1016/j.jhazmat.2011.05.024

duplicates or triplicates unless otherwise specified. SNPs were dispersed using an ultrasonic processor with a frequency of 132 kHz (Crest, USA). The extracellular proteins (ECPs) were extracted from the bacteria *A. punctata* (accession no. GQ401237) and *B. pumilus* (accession no. GQ401238) isolated from the sewage environment (Vellore, India). These organisms were previously reported as SNP resistant [18,19].

### 2.2. Extraction and characterization of ECP

The extraction and purification of bacterial ECP was performed according to the protocol described by Guo et al. [20]. The bacterial species were cultured in LB medium for 24 h at 28 °C. The cultures were centrifuged at 8000 × *g* for 10 min and the supernatants were collected. The supernatant was added with 90% ammonium sulfate and then centrifuged at 4 °C. The precipitate was dialyzed to remove salts and the crude protein was thus obtained. After the extraction the samples were subjected to sodium dodecyl sulfate-polyacrylamide gel electrophoresis (SDS-PAGE) [21].

### 2.3. Characterization of SNPs

SNPs were characterized using UV–visible spectroscopy (Schimadzu UV-1700, Japan), high resolution transmission electron microscopy (TEM, Tecnai G-20) and scanning electron microscopy (FEI Sirion, Eindhoven, Netherlands). A drop of nanoparticle suspension was deposited on a TEM grid, allowed to dry, rinsed, and directly observed with an electron microscope operated at 80 kV. Mean particle size was analyzed from the digitized images with Image Tool software. The morphological features of the manufactured silver nanoparticles were characterized by SEM. The size distribution of nanoparticles in aqueous dispersion of the particles was determined by dynamic light scattering method using a particle size analyser (90Plus Particle Size Analyzer, Brookhaven Instruments Corp., Holtsville, New York). The surface area was measured using a Smart Sorb 93 Single point BET surface area analyzer (Smart Instruments Co. Pvt. Ltd., Mumbai, India). The particles were also subjected to X-ray diffraction analysis using a JEOL-JDX 8030 difractometer. The target was Cu Kα (λ = 1.54 Å). The generator was operated as 45 kV and with a 30 mA current. The scanning range ($2\theta$) was selected from 10° to 100°.

### 2.4. Measurement of the zeta potential

The zeta potentials of SNPs and ECP were measured using a Brookhaven Zeta 90Plus analyzer. The SNPs and ECP were suspended in sterile distilled water and adjusted pH by 0.01 M HCl or NaOH solution. After the zeta potential measurements their exact pH values were measured again.

### 2.5. Adsorption isotherms

Adsorption isotherm experiments were carried out by adding a fixed amount of silver nanoparticles (20 mg/L) to a series of ECP concentrations (10–250 mg/L) at natural pH (pH value 7). The samples were stirred for 4 h in a rotary shaker at 200 rpm. The interaction was followed by centrifuging at 10,000 × *g* for 10 min. The supernatant was carefully collected and the ECP left in the supernatant was quantified by Lowery's method. The effect of pH on adsorption was investigated at room temperature and an initial concentration of 250 mg/L. The pH was adjusted using solutions of 0.1 M NaOH and 0.1 M HCl. The effect of salt (NaCl) concentration on adsorption was evaluated at different NaCl concentrations (0.05–1.5 M). The amount of ECP adsorbed at equilibrium '$q_e$' (mg/mg) on SNPs was calculated from the following equation:

$$q_e = \frac{(C_0 - C_e)V}{W} \quad (1)$$

where '$C_0$' and '$C_e$' (mg/L) are the concentrations of ECP at initial and equilibrium, respectively, '*V*' is the volume of the solution (L) and '*W*' is the mass of SNPs used (mg).

All the tests were carried out in triplicate, and mean values of the results were reported. The experimental error limit was strictly kept within ±5%.

After the interaction, the samples were lyophilized and subjected to X-ray diffraction (XRD) and Fourier-transform infrared spectroscopy (FTIR). Destabilization of ECP from SNPs was carried out at pH 12. For the desorption study, initially the SNPs were interacted with ECP at a concentration of 250 mg/L. Once equilibrium was reached, the interaction mixture was centrifuged and the ECP attached SNPs was separated out. Then the ECP adsorbed SNPs were washed by DI water. The SNPs containing ECP were then mixed with pH 12 solution. After 4 h of interaction, the supernatant was collected and the amount ECP desorbed from the SNPs was estimated.

### 2.6. Adsorption kinetics

Adsorption kinetics of ECP on SNPs was carried out with an initial concentration of 250 mg/L. Basically, the adsorption kinetic experiments were identical to those of isotherm experiments. At various time intervals, the suspensions were centrifuged and the concentration of ECP remains in the supernatant was determined. ECP concentration in supernatant was measured by Lowry's method. The amount of adsorption at time '*t*', '$q_t$' (mg/mg), was calculated by:

$$q_t = \frac{(C_0 - C_t)V}{W} \quad (2)$$

where '$C_0$' and '$C_t$' (mg/L) are the concentrations of ECP at initial and the time '*t*', respectively, '*V*' is the volume of the solution (L) and '*W*' is the mass of SNPs used (mg).

## 3. Results and discussion

### 3.1. Characterization of bacterial ECP

The molecular weight of the extracted proteins was determined by SDS-PAGE and was found to be between 15 and 98 kDa for both the bacterial species. Hirose et al. [22] reported that the bacterial extracellular production contains more than 180 proteins.

### 3.2. Characterization of SNPs

The size and morphology of SNPs were characterized by TEM and SEM. TEM image showed SNPs were spherical and polydispersed. The surface area of the manufactured SNPs was determined to be 0.26 $m^2$/g. UV–visible absorption spectra for SNPs showed absorption maximum at 425 nm. The particle size distribution analysis of SNPs showed an effective hydrodynamic diameter of 43 nm (Fig. 1). The XRD pattern of SNPs gave a major peak at 38.115 and minor peaks at 44.299, 64.443, 77.397, 81.541 and 98.241.

### 3.3. UV–visible spectral study

The UV–visible absorption band for SNPs was observed at 425 nm. A decrease in absorbance was observed for ECP concentrations of 10, 20, 30, 40 and 50 mg/L with no noticeable plasmon shift. A blue shift (towards lower wavelength) in absorbance value

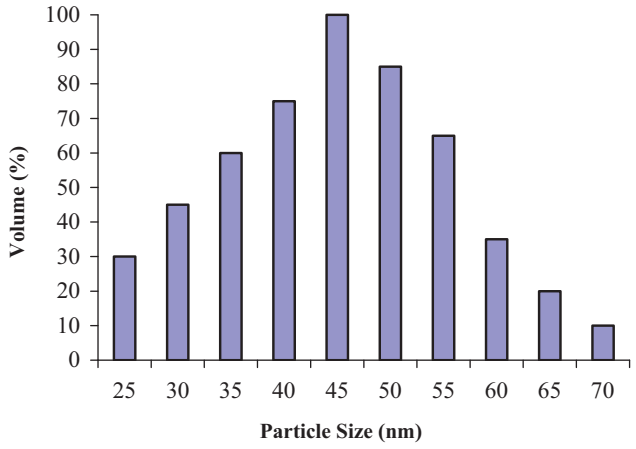


**Fig. 1.** Size distribution of SNPs obtained from dynamic light scattering method.

of SNPs (425 nm) was observed above 50 mg/L ECP concentration. The lowest absorbance value was noted at 417 nm. The blue shift may be attributed to the enhanced electrostatic repulsion due to electron density on the particle surfaces. The negatively charged ECP will restrict the free electrons of the SNPs within a smaller volume leading to an increased free electron density, thus a higher plasmon frequency (lower wavelength).

### 3.4. Influence of pH

The pH of the interaction solution influences the adsorption capacity of ECP on to SNPs (Fig. 2a). There was not much difference in the adsorption capacity of ECP on SNPs with an increase in pH from 4 to 8. When the pH was adjusted to 9, the amount of adsorbed ECP on SNPs decreased. A possible explanation for pH effect on adsorption may be related to the surface charge of the nanoparticles and ECP. Fig. 2b shows the surface charge of ECPs and SNPs at different pH values. The results show that the zeta potential of ECP produced by both the bacterial species was negatively charged in all pH values tested. On the other hand SNPs have positive charge up to pH 8 and negative charge at above pH 8. This zeta potential value agrees well with the adsorption mechanism. In the case of pH >8, the electrostatic force is large due to the negatively charged surface of both SNPs and ECPs and therefore, the electrostatic repulsion does not favor the adsorption of ECP on SNPs. In pH values below 8, it is shown that electrostatic interaction is one of the driving forces for the adsorption of ECP on the SNPs. In this region, ECP has a negative charge while SNPs have a positive charge, the electrostatic repulsion between SNPs and ECP is weak, which can promote the adsorption of ECP on SNPs. Therefore, it is not surprising that negative charge ECP molecules are easily adsorbed on the surface of SNPs at a low pH range (<8) due to strong electrostatic attraction between ECPs and SNPs. The results suggested that the environmental pH would favor the adsorption of ECP on SNPs.

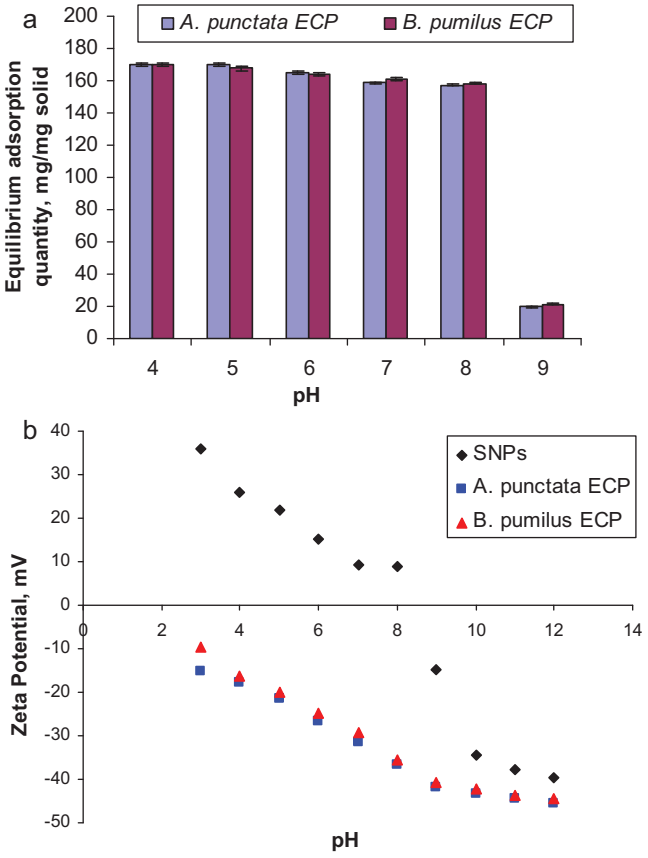


**Fig. 2.** (a) Effect of pH on adsorption of ECP on SNPs. (b) Zeta potential of the ECPs and the nanoparticles at different pH values.

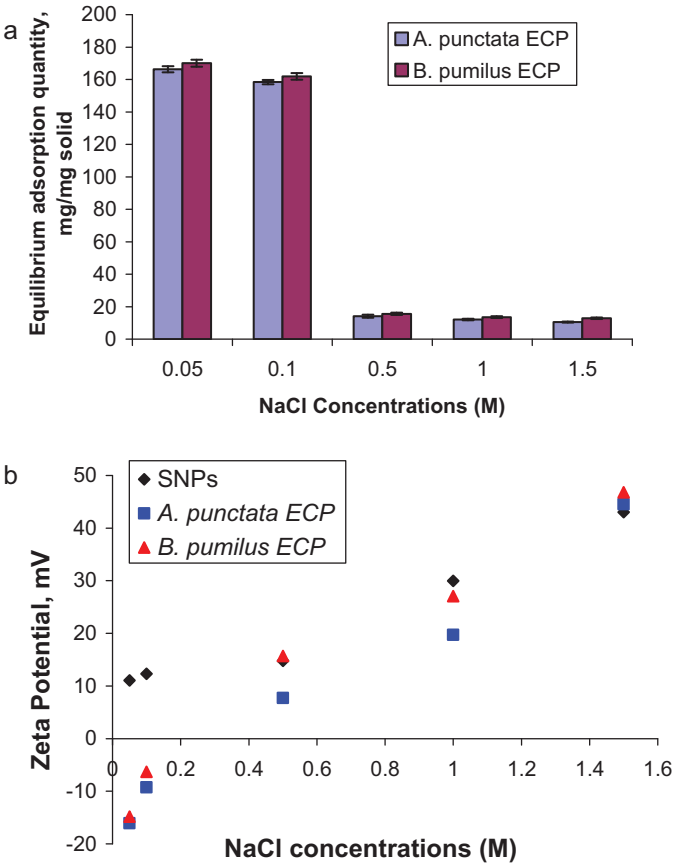


**Fig. 3.** (a) Effect of salt (NaCl) concentrations on adsorption. (b) Zeta potential of the ECPs and SNPs at different salt (NaCl) concentrations.

### 3.5. Influence of salt (NaCl) concentration

The salt concentration of the interaction solution is also an important parameter influencing the adsorption capacity of ECP on SNPs. Fig. 3a shows the effect of salt concentration on the adsorption of ECP on SNPs with a feed concentration of 250 mg/L ECP. Results show that when salt concentration was increased from 0 to 0.1 M, there was no significant change on adsorption observed. The

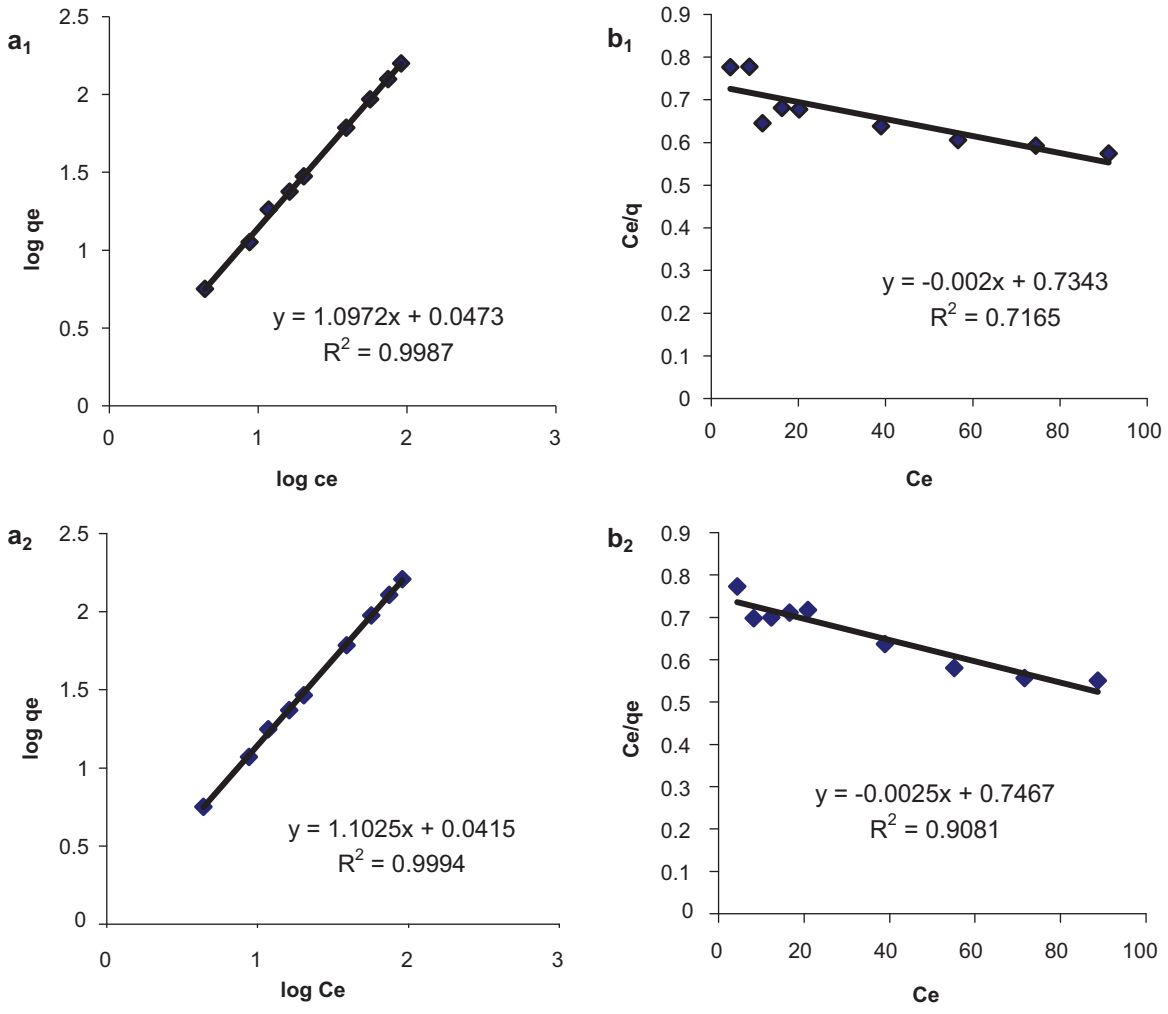


**Fig. 4.** Adsorption isotherm of ECP on SNPs. Figure $a_1$ and $b_1$ represents the Freundlich and Langmuir isotherm models of ECP extracted from *A. punctata* and figure $a_2$ and $b_2$ represents the Freundlich and Langmuir isotherm models of ECP extracted from *B. pumilus* respectively.

adsorption capacity was drastically decreased, when NaCl concentration was beyond 0.1 M. It is proposed that high concentrations of NaCl ions could cover the particle surface and form an ion shield, which can decrease the adsorption capacity of ECP on SNPs [23]. A possible explanation for the difference in adsorption may be related to the surface charge of nanoparticles and ECP. The surface charge of ECPs and SNPs at different salt concentrations was determined (Fig. 3b). The results show that the zeta potential of ECP was negative up to 0.1 M NaCl concentration and above which it turned to positive charge. SNPs exhibited positive charge at all salt concentrations tested. At above 0.1 M NaCl concentrations, the electrostatic force is large due to the positively charged surface of both SNPs and ECPs, and therefore, the electrostatic repulsion does not favor the adsorption of ECP on SNPs. Below 0.1 M NaCl concentrations, the electrostatic repulsion is weak; the negative charge of ECP was adsorbed onto the positively charged SNPs.

### 3.6. Adsorption isotherms

Adsorption capacity at different aqueous equilibrium concentration can be explained by the adsorption isotherm studies. The adsorption process is normally described by the Freundlich and the Langmuir isotherms. The adsorption data were fitted to linearized forms of both Freundlich and Langmuir isotherms to find out the optimum isotherm relationship. Fig. 4 shows adsorption isotherms for ECP extracted from *A. punctata* and *B. pumilus* on SNPs surface at pH 7 and room temperature. In this study ECPs and SNPs were the adsorbate and adsorbent respectively.

The Freundlich adsorption isotherm model assumes the multilayer of adsorption on particle surfaces. The Freundlich equation is an empirical equation and can be expressed as follows:

$$q_e = K_F C_e^{1/n} \quad (3)$$

where '$C_e$' is the mass concentration of ECP in the supernatant (mg/L), '$q_e$' is the amount of ECP (mg) adsorbed per mg of SNPs in equilibrium, '$K_F$' is the Freundlich constant (mg/mg)(L/mg)$^{1/n}$. A linear form of the Freundlich expression can be obtained by taking logarithms of Eq. (3):

$$\log\ q_e = \frac{1}{n}\log C_e + \log K_F \quad (4)$$

Fig. 4a shows the plot of '$\log q_e$' versus '$\log C_e$', enables the constant '$K_F$' and exponent $1/n$ to be determined. The Freundlich isotherm constants were also manually calculated solving the simultaneous equations. The Freundlich isotherm describes multilayer of adsorption and is not restricted to the formation of the monolayer. The Freundlich equation predicts that the ECP concentration on the adsorbent will increase so long as there is an increase in the ECP concentration in the interaction medium. Our experimental data fit well with Freundlich isotherm model, suggesting the multilayer adsorption of ECP on SNPs surface. The high '$R^2$' values (linear regression coefficients) indicate that the Freundlich model

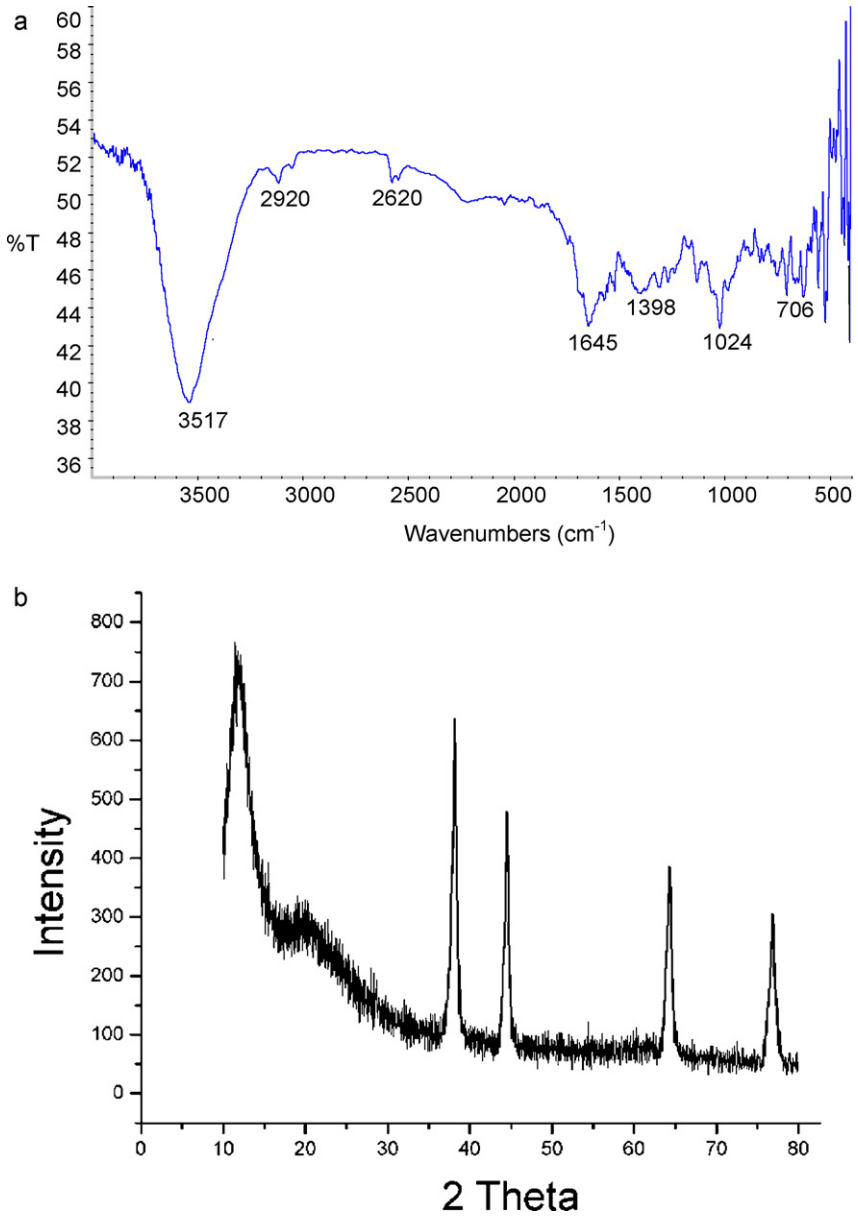


**Fig. 5.** (a) Represents the FTIR spectrum and (b) represents the XRD pattern of the *A. punctata* ECP adsorbed SNPs. The similar kinds of results were observed with *B. pumilus* ECP adsorbed SNPs (figure not shown).

predicts well the adsorption behavior of ECP on SNPs than Langmuir model. The results show that the Freundlich isotherm can fit the equilibrium data for adsorption of ECP on SNP surface.

The Langmuir equation assumes that once a molecule occupies a site, no further adsorption can take place at that site. The Langmuir equation is expressed as follows:

$$q = \frac{q_{max} \cdot K_a \cdot C_e}{1 + K_a \cdot C_e} \quad (5)$$

where '$C_e$' is the mass concentration of ECP in the supernatant (mg/L), '$q_e$' is the amount of ECP (mg) adsorbed per mg of SNPs, '$q_{max}$' is the maximum amount of ECP at SNPs surface for a monolayer and '$K_a$' is the adsorption constant (L/mg), reflects the affinity of ECP for SNP surface. Eq. (5) can be rearranged to a linear form:

$$\frac{C_e}{q_e} = \frac{1}{q_{max} K_a} + \frac{C_e}{q_{max}} \quad (6)$$

The constants '$q_{max}$' and '$K_a$' were calculated from the intercepts and the slopes of the linear plots of '$C_e/q_e$' versus '$C_e$' (Fig. 4b). The Langmuir isotherm constants were also manually calculated. The large variations between the graphical solution, and analytical solutions indicated that the experimental data did not fit well in Langmuir model.

The FTIR analysis was carried out to identify the possible interactions between the SNPs and ECPs (Fig. 5a). Amide I and Amide II are the most important bands of the protein infra red spectrum [24]. The bands obtained at 3500 $cm^{-1}$ and between 1600 and 1700 $cm^{-1}$ indicated the Amide groups confirming adsorption of ECP. This parallels to the study of Lu et al. [25] and Ravindran et al. [26] that nanoparticles interact with the protein molecules at specific binding sites. The functional groups present in the ECP provide abundant binding ligands for the nanoparticles [27,28]. In FTIR analysis the characteristic bands of ECP were observed with lyophilized SNPs after interaction with ECP suggests that, the ECP was successfully attached to the surface of SNPs. The ECP can stabilize nanoparticle dispersions and thus enhance toxicity of the nanoparticles [29]. The XRD spectrum shows the characteristic peak for SNPs after interaction with ECP confirms the crystallinity of nanoparticles (Fig. 5b).

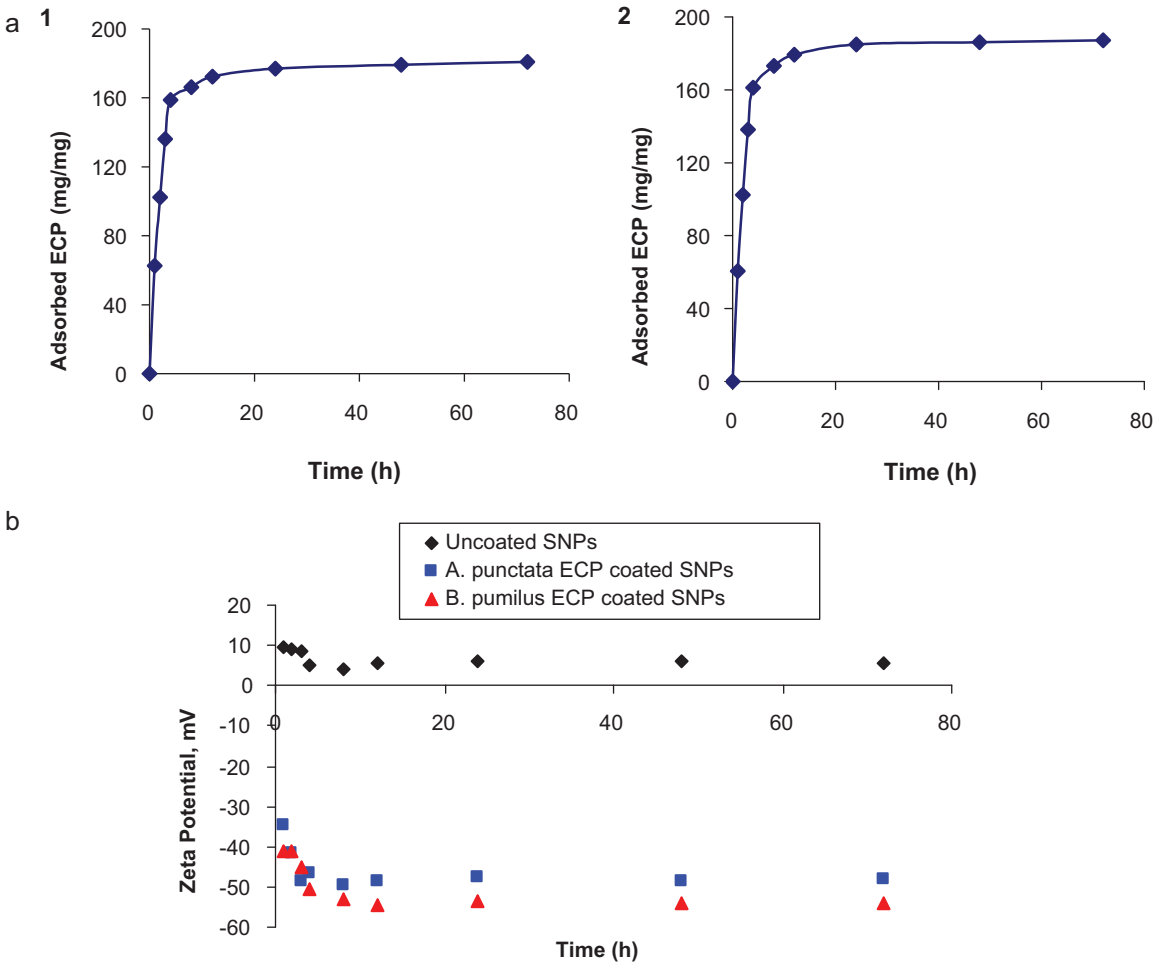


**Fig. 6.** (a) The adsorption kinetics of ECP on SNPs at an initial concentration of 250 mg/L. Figure $a_1$ and $a_2$ represents the adsorption kinetics of ECP extracted from *A. punctata* and *B. pumilus* respectively. (b) The zeta potential of ECP adsorbed SNPs over the interaction period (72 h).

There may be many mechanistic principles of binding of nanoparticles to protein molecules, of which the most understood is "end on" or "side-on" binding, in which end-on binding results in a higher surface coverage of protein on the surface of nanoparticles [30]. Proteins are attached to the surface of nanoparticles by chemical cross-linking or due to electrostatic force of attraction. The binding of a protein to the surface of a particle is achieved by electrostatic interactions [30]. Reactivity of individual amino acids or functional groups with nanoparticles may also impart in binding [31–33].

Wigginton et al. [34] reported the probable mechanism of adsorption of bacterial protein on the surface of SNPs and their study highlights the potential effect of nanoparticle surface coating on bioavailability. Some studies revealed the role of biomolecules in SNP toxicity and its bioavailability [15]. Similar results could be observed from organically and inorganically coated nanoparticles once they are released into the environment. Ng et al. [35] reported that SNPs are ideal for incorporation into the membranes in order to reduce the biofouling of the polymeric membranes. These polymer coated SNPs are found to be stable in the environment and exhibited higher toxicity to bacterial species [36]. There were some reports on the stabilization of nanoparticles in the environment by humic acid and these stable nanoparticles were able to disrupt the bacterial biofilm and natural aquatic bacterial assemblage [14,37]. Luo et al. [38] reported that the toxicity of nanoparticle is related to surface properties and the nanoparticles can be functionalized with a monolayer or multiplayer assembly of the desired hydrophobic or hydrophilic functional groups. The nanocomposite material based on lactose modified chitosan and SNPs found to have high toxicity to gram positive and gram negative bacterial species [39]. Fabrega et al. [40] evaluated the behavior, the biological effects and the route of uptake of SNPs to organisms and reported that very low concentration (ng/L) of SNPs can significantly affect prokaryotes, invertebrates and fish.

### 3.7. Adsorption kinetics

The adsorption kinetics is important for adsorption studies because it can predict the rate at which the ECP adsorbed on the surface of SNPs from aqueous solutions and provides valuable data for understanding the mechanism of adsorption reactions. In order to investigate the mechanism of adsorption and the potential rate controlling steps, such as mass transport and chemical reaction processes, two simple kinetic models *viz*. the pseudo-first-order [41] and pseudo-second -order [42] have been used to test experimental data of ECP aqueous solutions. Here we have investigated the adsorption kinetics for ECP extracted from *A. punctata* and *B. pumilus* on SNP surface at pH 7 and room temperature. The adsorption kinetics was carried out at an initial concentration of 250 mg/L ECP and the results are shown in Fig. 6a. In most of the cases, the stability of nanoparticles is mainly depending on the surface charge. The high negative or positive charge surface will repel each other due to electrostatic force of repulsion. Here, we have determined the zeta potential of ECP capped SNPs over the interaction period

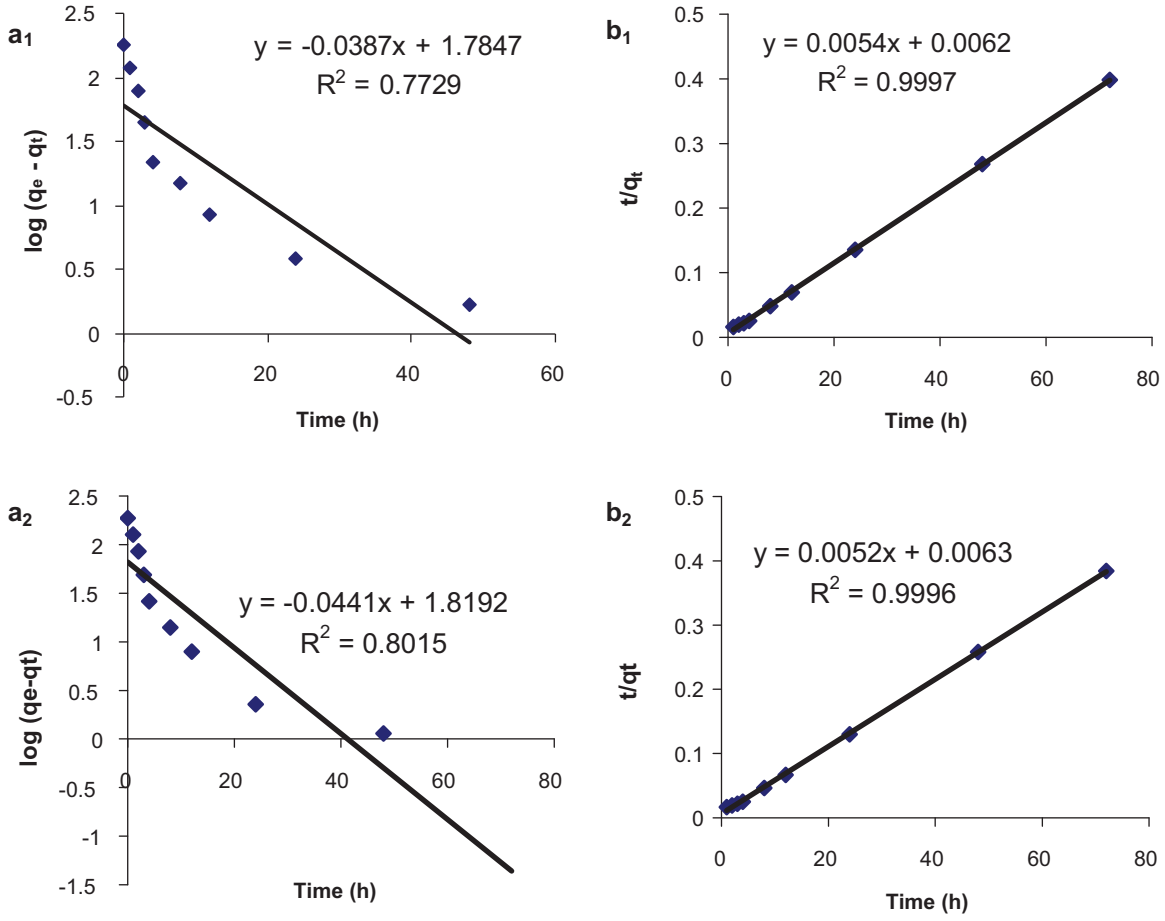


**Fig. 7.** (a) The pseudo-first-order kinetics plotted as a function of $\log(q_e - q_t)$ versus time (h) and (b) the pseudo-second-order kinetics plotted as a function of $t/q_t$ versus time (h). Figure $a_1$ and $b_1$ represents the pseudo-first-order kinetics and pseudo-second-order kinetics of ECP extracted from *A. punctata* and figure $a_2$ and $b_2$ represents the pseudo-first-order kinetics and pseudo-second-order kinetics of ECP extracted from *B. pumilus* respectively.

(Fig. 6b). The zeta potential less than −30 mV and greater than +30 is considered as stable due to the high electrostatic force of repulsion. The study suggests that the SNPs are highly stable and it exhibited the zeta potential of less than −30 mV over the interaction period (72 h) indicates the stability of ECP capped SNPs.

Linear form of pseudo-first-order kinetic equation is expressed as

$$\log(q_e - q_t) = \log q_e - \frac{k_1}{2.303} t \quad (7)$$

where '$q_e$' and '$q_t$' are the amounts of adsorbed ECP on SNPs at equilibrium and at time '$t$' (mg/L), respectively, and '$k_1$' is the equilibrium rate constant of pseudo-first-order adsorption. The slope and intercept of the plot, '$\log(q_e - q_t)$' versus '$t$' were used to obtain the pseudo-first-order rate constant '$k_1$' and equilibrium adsorption density '$q_e$'. The '$R^2$' values obtained are relatively small and the experimental '$q_e$' values do not agree with the calculated values obtained from the linear plots (Fig. 7a).

Linear form of pseudo-second-order kinetic equation is expressed as

$$\frac{t}{q_t} = \frac{1}{k_2(q_e)^2} + \frac{t}{q_e} \quad (8)$$

The second order rate constant '$K_2$' and '$q_e$' values were determined from the slopes and intercepts of the plots. The correlation coefficients '$R^2$' value is the indicative of the strength of the linear relationship. The linear plot of '$t/q_t$' versus '$t$' is shown in Fig. 7b and the obtained '$R^2$' values are greater than 0.999 for both the ECP samples. The theoretical '$q_e$' values agree well with the experimental '$q_e$' values, suggesting the adsorption data tend to follow pseudo-second-order kinetics. For desorption studies more than 90% desorption was observed at pH 12.

## 4. Conclusion

The release of nanomaterials in the environment leads to the interaction with biological molecules. The present study reports that the interaction of nanomaterials with bacterial ECP stabilizes the nanoparticles and possibly this might increase the hazardous potential of nanoparticles in the environment. The ECP capped nanoparticles were found to be stable at environmental pH and salt concentration; it might lead to the accumulation and transport of nanomaterials in the environment. The stable nanoparticles disrupt the microbial and algal communities, possibly affect the human beings and ultimately they destabilize the ecosystem functioning. Further studies are required to characterize the extracellular protein produced by bacterial species.

## Acknowledgements

Authors thank VIT University Chancellor, for providing us with funding to carry out our research.

## References

[1] The Royal Society & The Royal Academy of Engineering, Nanoscience and Nanotechnologies: Opportunities and Uncertainties, 2004.

[2] F. Furno, K.S. Morley, B. Wong, B.L. Sharp, P.L. Arnold, S.M. Howdle, et al., Silver nanoparticles and polymeric medical devices: a new approach to prevention of infection? J. Antimicrob. Chemother. 54 (2004) 1019–1024.
[3] C.F. Chau, S.H. Wu, G.C. Yen, The development of regulations for food nanotechnology, Trends Food Sci. Technol. 18 (2007) 269–280.
[4] I. Perelshtein, G. Applerot, N. Perkas, G. Guibert, S. Mikhailov, A. Gedanken, Sonochemical coating of silver nanoparticles on textile fabrics (nylon, polyester and cotton) and their antibacterial activity, Nanotechnology 19 (2008) 245705.
[5] D Roe, B. Karandikar, N.B. Savage, B. Gibbins, J.B. Roullet, Antimicrobial surface functionalization of plastic catheters by silver nanoparticles, J. Antimicrob. Chemother. 61 (2008) 869–876.
[6] M. Das, N. Saxena, P.D. Dwivedi, Emerging trends of nanoparticles application in food technology: safety paradigms, Nanotoxicology 3 (2009) 10–18.
[7] D.R. Monteiro, L.F. Gorup, A.S. Takamiya, A.C. Ruvollo, E.R. de-Camargo, D.B. Barbosa, The growing importance of materials that prevent microbial adhesion: antimicrobial effect of medical devices containing silver, Int. J. Antimicrob. Agents 34 (2009) 103–110.
[8] Woodrow Wilson Institute, Nanotechnology Consumer Product Inventory, http://www.nanotechproject.org/inventories/consumer/analysis_draft/, 2009.
[9] http://pubs.acs.org/cen/news/88/i39/8839news2.html.
[10] N.C. Mueller, B. Nowack, Exposure modeling of engineered nanoparticles in the environment, Environ. Sci. Technol. l42 (2008) 4447–4453.
[11] R. Paull, J. Wolfe, P. Herbert, M. Sinkula, Investing in nanotechnology, Nat. Biotechnol. 21 (2003) 1144–1147.
[12] S.M. Hussain, J.J. Schlager, Safety evaluation of silver nanoparticles: inhalation model for chronic exposure, Toxicol. Sci. 108 (2009) 223–224.
[13] P.V. AshaRani, G.L.K. Mun, M.P. Hande, S. Valiyaveettil, Cytotoxicity and genotoxicity of silver nanoparticles in human cells, ACS Nano 3 (2009) 279–290.
[14] T.P. Dasari, H.M. Hwang, The effect of humic acids on the cytotoxicity of silver nanoparticles to a natural aquatic bacterial assemblage, Sci. Total Environ. 408 (2010) 5817–5823.
[15] C.O. Dimkpa, A. Calder, P. Gajjar, S. Merugu, W. Huang, D.W. Britt, J.E. McLean, W.P. Johnson, A.J. Anderson, Interaction of silver nanoparticles with an environmentally beneficial bacterium, *Pseudomonas chlororaphis*, J. Hazard. Mater. (2011), doi:10.1016/j.jhazmat.2011.01.118.
[16] C.A. Impellitteri, T.M. Tolaymat, K.G. Scheckel, The speciation of silver nanoparticles in antimicrobial fabric before and after exposure to a hypochlorite/detergent solution, J. Environ. Qual. 38 (2009) 1528–1530.
[17] S. Blaser, M. Scheringer, M. MacLeod, K. Hungerbuhler, Exposure of modeling of nano silver in the environment, in: NanoECO Conference, Monte Verita, 2008.
[18] S Sudheer Khan, E. Bharath Kumar, A. Mukherjee, N. Chandrasekaran, Bacterial tolerance to silver nanoparticles (SNPs): *Aeromonas punctata* isolated from sewage environment, J. Basic Microbiol. 50 (2010) 1–8.
[19] S. Khan, A. Mukherjee, N. Chandrasekaran, Silver nanoparticles tolerant bacteria from sewage environment, J. Environ. Sci. 23 (2011) 346–352.
[20] S.H. Guo, J.K. Chen, W.C. Lee, Purification and characterization of extracellular chitinase from *Aeromonas schubertii*, Enzyme Microb. Technol. 35 (2004) 550–556.
[21] http://www.nature.com/nprot/journal/v1/n1/full/nprot.2006.4.html.
[22] I. Hirose, K. Sano, I. Shioda, M. Kumano, K. Nakamura, K. Yamane, Proteome analysis of *Bacillus subtilis* extracellular proteins: a two-dimensional protein electrophoretic study, Microbiology 146 (2000) 65–75.
[23] H. Liu, Y. Wang, W. Chen, The sorption of lysozyme and ribonuclease onto ferromagnetic nickel powder. 1. Adsorption of single components, Colloids Surf. B 5 (1995) 25–34.
[24] A. Papadopoulou, R.J. Green, R.A. Frazier, Interaction of flavonoids with bovine serum albumin: a fluorescence quenching study, J. Agric. Food Chem. 53 (2005) 158–163.
[25] X. Lu, S. Cui, Wool keratin-stabilized silver nanoparticles, Bioresour. Technol. 101 (2010) 4703–4707.
[26] A. Ravindran, A. Singha, A.M. Raichur, N. Chandrasekaran, A. Mukherjee, Studies on interaction of colloidal Ag nanoparticles with bovine serum albumin (BSA), Colloids Surf. B 76 (2010) 32–37.
[27] L.T. Salgado, L.R. Andrade, G.M. Amado, Localization of specific monosaccharides in cells of the brown alga *Padina gymnospora* and the relation to heavy-metal accumulation, Protoplasma 225 (2005) 123–128.
[28] A. Miao, K.A. Schwehr, C. Xu, S. Zhang, Z. Luo, A. Quigg, P.H. Santschi, The algal toxicity of silver engineered nanoparticles and detoxification by exopolymeric substances, Environ. Pollut. 157 (2009) 3034–3041.
[29] K.J. Wilkinson, A. Reinhardt, Contrasting roles of natural organic matter on colloidal stabilization and flocculation in freshwaters, in: I.G. Droppo, G.G. Leppard, S.N. Liss, T.G. Milligan (Eds.), Flocculation in Natural and Engineered Environmental Systems, CRC Press, Boca Raton, FL, 2005, pp. 143–170.
[30] E.W. Stein, M.J. McShane, Multilayer lactate oxidase shells on colloidal carriers as engines for nanosensors, IEEE Trans. Nanobiosci. 2 (2003) 133–137.
[31] S. Stewart, P.M. Fredericks, Surface-enhanced Raman spectroscopy of peptides and proteins adsorbed on an electrochemically prepared silver surface, Spectrochim. Acta Part A 55 (1999) 1615–1640.
[32] E. Podstawka, Y. Ozaki, L.M. Proniewicz, Adsorption of S–S containing proteins on a colloidal silver surface studied by surface-enhanced Raman spectroscopy, Appl. Spectrosc. 58 (2004) 1147–1156.
[33] E. Podstawka, Y. Ozaki, Surface-enhanced Raman difference between bombesin and its modified analogues on the colloidal and electrochemically roughen silver surfaces, Biopolymers 89 (2008) 807–819.
[34] N.S. Wigginton, A. DeTitta, F. Piccapietra, J. Dobias, V.J. Nesatyy, M.J.F. Suter, R.B. Latmani, Binding of silver nanoparticles to bacterial proteins depends on surface modifications and inhibits enzymatic activity, Environ. Sci. Technol. 44 (2010) 2163–2168.
[35] L.Y. Ng, A.W. Mohammad, C.P. Leo, N. Hilal, Polymeric membranes incorporated with metal/metal oxide nanoparticles: a comprehensive review, Desalination (2010), doi:10.1016/j.desal.2010.11.033.
[36] A.M. El-Badawy, R.G. Silva, B. Morris, K.G. Scheckel, M.T. Suidan, T.M. Tolaymat, Surface charge-dependent toxicity of silver nanoparticles, Environ. Sci. Technol. 45 (2011) 283–287.
[37] J. Fabrega, J.C. Renshaw, J.R. Lead, Interactions of silver nanoparticles with *Pseudomonas putida* biofilms, Environ. Sci. Technol. 43 (2009) 9004–9009.
[38] J. Luo, W.B. Chan, L. Wang, C.J. Zhong, Probing interfacial interactions of bacteria on metal nanoparticles and substrates with different surface properties, Int. J. Antimicrob. Agents 36 (2010) 549–556.
[39] A. Travan, E. Marsich, I. Donati, M. Benincasa, M. Giazzon, L. Felisari, S. Paoletti, Silver–polysaccharide nanocomposite antimicrobial coatings for methacrylic thermosets, Acta Biomater. 7 (2011) 337–346.
[40] J. Fabrega, S.N. Luoma, C.R. Tyler, T.S. Galloway, J.R. Lead, Silver nanoparticles: behaviour and effects in the aquatic environment, Environ. Int. 37 (2011) 517–531.
[41] S. Lagergren, About the theory of so-called adsorption of soluble substances, Kungliga Svenska Vetenskapsakademiens Handlinger 24 (1898) 1–39.
[42] Y.S. Ho, G. McKay, Pseudo-second order model for sorption processes, Process Biochem. 34 (1999) 451–456.